Review Article

New Components for Dye-Sensitized Solar Cells

Stefano Caramori,[1] Vito Cristino,[1] Rita Boaretto,[1] Roberto Argazzi,[2] Carlo Alberto Bignozzi,[1] and Aldo Di Carlo[3]

[1] *Dipartimento di Chimica, Università degli Studi di Ferrara, Via L. Borsari 46, 44100 Ferrara, Italy*

[2] *Dipartimento di Chimica, Istituto per la Sintesi Organica e la Fotoreattività (ISOF-CNR) c/o, Università degli Studi di Ferrara, Via L. Borsari 46, 44100 Ferrara, Italy*

[3] *Dipartimento di Ingegneria Elettronica, Università di Roma "Tor Vergata", Via del Politecnico 1, 00133 Roma, Italy*

Correspondence should be addressed to Carlo Alberto Bignozzi, g4s@unife.it

Dye-Sensitized Solar Cells (DSSCs) are among the most promising solar energy conversion devices of new generation, since coupling ease of fabrication and low cost offer the possibility of building integration in photovoltaic windows and facades. Although in their earliest configuration these systems are close to commercialization, fundamental studies are still required for developing new molecules and materials with more desirable properties as well as improving our understanding of the fundamental processes at the basis of the functioning of photoactive heterogeneous interfaces. In this contribution, some recent advances, made in the effort of improving DSSC devices by finding alternative materials and configurations, are reviewed.

1. Introduction

Dye-sensitized solar cells (DSSCs) are photoelectrochemical solar devices, currently subject of intense research in the framework of renewable energies being low-cost photovoltaic devices. DSSCs are based on the sensitization to visible light of mesoporous, nanocrystalline metal oxide films achieved by means of the adsorption of molecular dyes [1–3]. Photoinduced electron injection from the sensitizer dye (D) into the metal oxide conduction band initiates charge separation. Subsequently, the injected electrons are transported through the metal oxide film to a transparent electrode, while a redox-active electrolyte, such as I_3^-/I^-, is employed to reduce the dye cation and transport the resulting positive charge to a counter electrode (Figure 1).

DSSCs efficiencies up to 10.4% [4] have been reported for devices employing nanocrystalline TiO_2 films. Several studies have addressed the use of alternative metal oxides including SnO_2 [5, 6], ZnO [7, 8], and Nb_2O_5 [9]. The performance of dye-sensitized solar cells can be understood in view of the kinetic competition among the various redox processes involved in the conversion of light into electricity. Ultrafast electron injection (k_2) has been observed in the femtosecond-picosecond (10^{-15}–10^{-12} s) time domain. Regeneration of the oxidized dye (k_4) is typically characterized by rate constants of 10^7–10^9 s^{-1}. This is more than 100 times faster than recombination of injected electrons with the oxidized redox species (k_6) and orders of magnitude faster than back transfer to the dye cation in the absence of a redox mediator (k_3). As electron transport in the semiconductor electrode is generally one order of magnitude faster than recombination, the charge collection efficiency is near unit for optimized cells. Because of the prevailing role of electron transfer dynamics in DSSCs, the various processes have been widely studied in the last decade. While photo-electrochemical techniques proved to be most adequate for the study of electron transport, time-resolved optical spectroscopy remains the leading tool for the study of interfacial electron transfer. Dye regeneration and back transfer reactions have been intensely studied by nanosecond laser spectroscopy. On the other hand, due to its astonishing rate, the forward electron transfer reaction remained unresolved for several years: the advent of femtosecond laser spectroscopy opened the door to the domain of ultrafast chemical processes.

$k_1 = (10^8 - 10^{10}) \, \mathrm{s}^{-1}$
$k_2 = (10^{10} - 10^{12}) \, \mathrm{s}^{-1}$
$k_3 = (10^6 - 10^7) \, \mathrm{s}^{-1}$
$k_4 = (10^8 - 10^9) \, \mathrm{s}^{-1}$
$k_5 = (10^0 - 10^2) \, \mathrm{s}^{-1}$
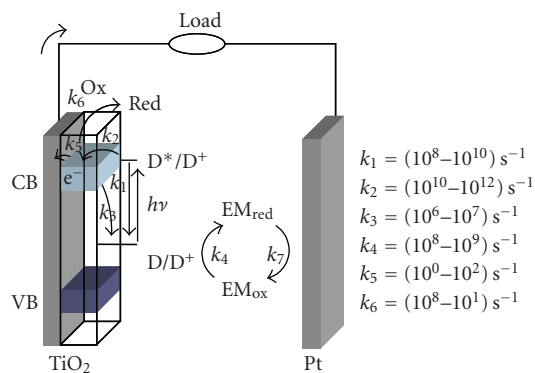$k_6 = (10^8 - 10^1) \, \mathrm{s}^{-1}$

Figure 1: Electron transfer processes involved in a DSSC and their time scale.

The functioning of DSSCs is the interlacing of several subsystems which should work in tandem: the dye sensitizer, that is, the dye adsorbed on the semiconductor surface able to absorb the visible and near-IR photons and to pump electrons into the conducting band of semiconductor, the electron mediator for "hole", conduction and the counter electrode catalytic materials. We report here on the recent advances in the design of these DSSC components.

2. Molecular Sensitizers

One of the most important DSSC component, is the dye sensitizer, which represents the photodriven elctron pump of the device. It allows an independent electron injection into the semiconductor conduction band and conversion of visible and near infrared photons to electricity.

Several organic and inorganic compounds have been investigated for semiconductor sensitization, such as chlorophyll derivatives [10], porphyrins [11], phtalocyanines [12, 13], platinum complexes [14, 15], fluorescent dyes [16], carboxylated derivatives of anthracene [17], polymeric films [18], and coupled semiconductors with lower-energy bandgaps [19], among others.

The best solar to electric power conversion efficiency has been achieved with polypyridyl complexes of ruthenium(II) [20] and osmium(II) [21] bearing carboxylated ligands, which are often employed as TiO_2 sensitizers in such cells. These species give rise to intense visible metal-to-ligand charge transfer (MLCT) bands with a favourable energetics for activationless charge injection. Among this family of compounds, excellent results have been achieved with thiocyanate derivatives. In particular, the performances of the Ru(II)-NCS complexes (Figure 2). In photoelectrochemical solar cells were found to be outstanding [20, 22]. The complexes show photoaction spectra dominating almost the entire visible region, short-circuit photocurrents exceeding $16 \, \mathrm{mA/cm^2}$ under simulated A.M. 1.5, sunlight and open-circuit photovoltages of the order of $0.7 \, \mathrm{V}$ in the presence of I_3^-/I^- as redox electrolyte. Their high efficiency is related to hole delocalization across the NCS ligands [23, 24] which is responsible for an increased electronic coupling of the

electron transfer reaction involving $TiO_2/Ru^{III}NCS$ and I^-. This leads to an increase of the rate constant of the reductive process (k_4, in Figure 1) and, as a consequence, of the IPCE (Incident Photon to Carrier Efficiency).

The photoelectrochemical performances obtained with the mononuclear complex $[Ru(dcbH_2)_2(NCS)_2]$ have been surpassed by an analogous species based on the terpyridine ligand [4]. Indeed, TiO_2 electrodes covered with the complex $Ru(L)(NCS)_3$ (L = 4,4′,4″-tricarboxy-2,2′:6′,2″-terpyridine) in its monoprotonated form displayed very efficient panchromatic sensitization covering the whole visible spectrum and extending the spectral response to the near IR region, up to 920 nm, with maximum IPCE values comparable to that obtained with the dithiocyanate complex. The panchromatic efficiency has been further extended in a series of cationic dyes, corresponding to the general formulae $[M(H_3tcterpy)LY]^+$ [25]: M = Os(II) or Ru(II); ($H_3tcterpy$) is the tridentate ligand, 4,4′,4″-tricarboxy-2,2′:6′,2″-terpyridine, and L is a bidentate ligand of the type (bpy, 2,2′-bipyridine) or (pyq, 2-2′-pyridylquinoline) (Figure 3), which can be substituted both in the 4 and 4′ positions by X = H, CH_3, COOH, or $C(CH_3)_3$, and Y = Cl^-, I^-, or NCS^-. These dyes show reversible metal oxidations and, in the Os case, unprecedented photoconversion efficiency in the near infrared (NIR), approaching in the best case the value of 50% at 900 nm.

Many attempts to replace the thiocyanate donor ligands have been made, because the monodentate NCS^- is believed to be the weakest part of the complexes from the chemical stability point of view. Recently a novel thiocyanate-free cyclometalated ruthenium complex containing the 2-(2,4-Difluorophenyl)pyridine has been observed to produce a remarkable incident monochromatic photon-to-current conversion efficiency of 83% [26]. The solar cell employing a liquid-based electrolyte exhibits a short circuit photocurrent density of $17 \, \mathrm{mA/cm^2}$, an open circuit voltage of 800 mV, and a fill factor of 0.74, corresponding to an overall conversion efficiency of 10.1% at standard AM 1.5 sunlight.

Besides metal organic dyes, relevant efforts are currently being directed towards the synthesis of novel types of ruthenium-free organic dye sensitizers which display intense visible bands and favourable ground and excited state energetics. Usually the organic dye efficiency is lower than that displayed by MLCT complexes, but considerable success has been recently met with a careful synthetic design of chlorophylls [27] push-pull porphyrins [26, 28], phtalocyanins [29], and some squaraine dyes [30], particularly suited to harvest the NIR portion of the solar spectrum.

Fruit and vegetable extracts have also been used as natural sensitizers in photoelectrochemical solar cells [31, 32]. The interest in natural dyes arises from the possibility of achieving an efficient sensitization without expensive and time consuming synthetic and purification procedures. Among raw natural dyes, cyanines and betalains have achieved maximum monochromatic photon to electron conversions exceeding 60% and short circuit photocurrents approaching $10 \, \mathrm{mA/cm^2}$, under $0.1 \, \mathrm{W/cm^2}$ simulated solar irradiation. Red turnip, wild prickly pear, and eggplant were identified, up to now, as, respectively, the best natural sources
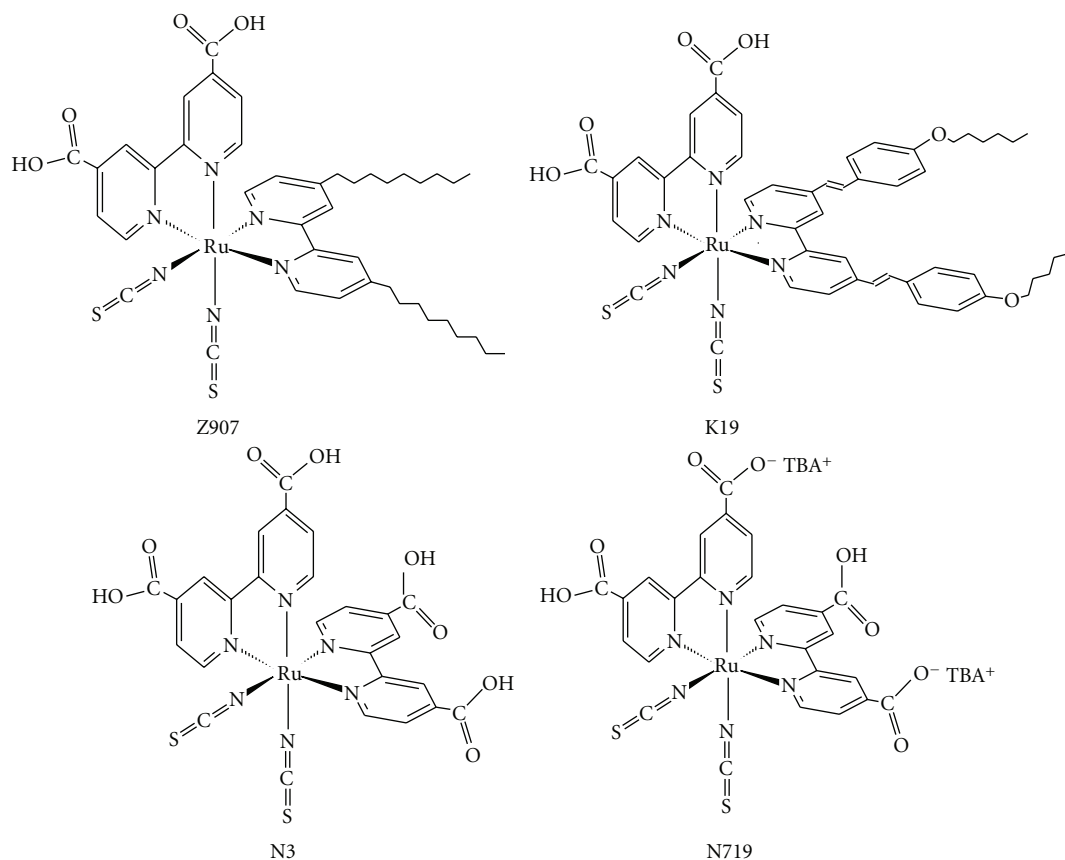
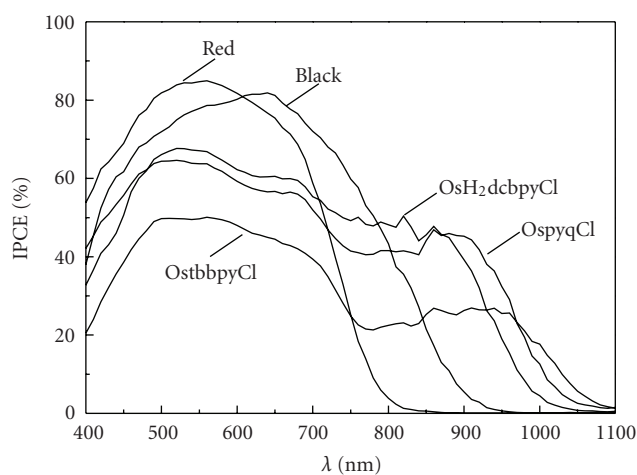FIGURE 2: Structure of some of the most successful polypyridine Ru(II) dye based on the NCS ancillary ligand.

FIGURE 3: Photoaction spectra of Os dyes measured in sandwich type solar cells (nanocrystalline TiO_2 films, electrolyte made of 2 M $LiI + 0.1$ M I_2 in γ-butyrolactone). $OsH_2dcpyCl = [Os(H_3tcterpy)(H_2dcbpy)(Cl)]^+$; $OstbbpyCl = [Os(H_3tcterpy)(tbbpy)(Cl)]^+$; $OspyqCl = [Os(H_3tcterpy)(pyq)(Cl)]^+$. Red and black dye are N3 and $Ru(H_3Tcterpy)(NCS)_3^-$, respectively.

of betalain and antocyanines pigments for TiO_2 sensitization (Figure 4).

In general, the natural dyes tested so far suffer from low Voc (440–480 mV) which is at best 100 mV lower than an equivalent N 719 sensitized cell. This can be due to possible efficient electron/dye cation recombination pathways and to the acidic dye adsorption environment. In fact, it is necessary an acidic environment to obtain a satisfactory dye coverage of the semiconductor surface and it is well known that H^+ are potential determining ions for TiO_2 causing a positive shift of the Fermi level of the TiO_2 and limiting the maximum photovoltage that can be delivered by the cells. Electron/dye
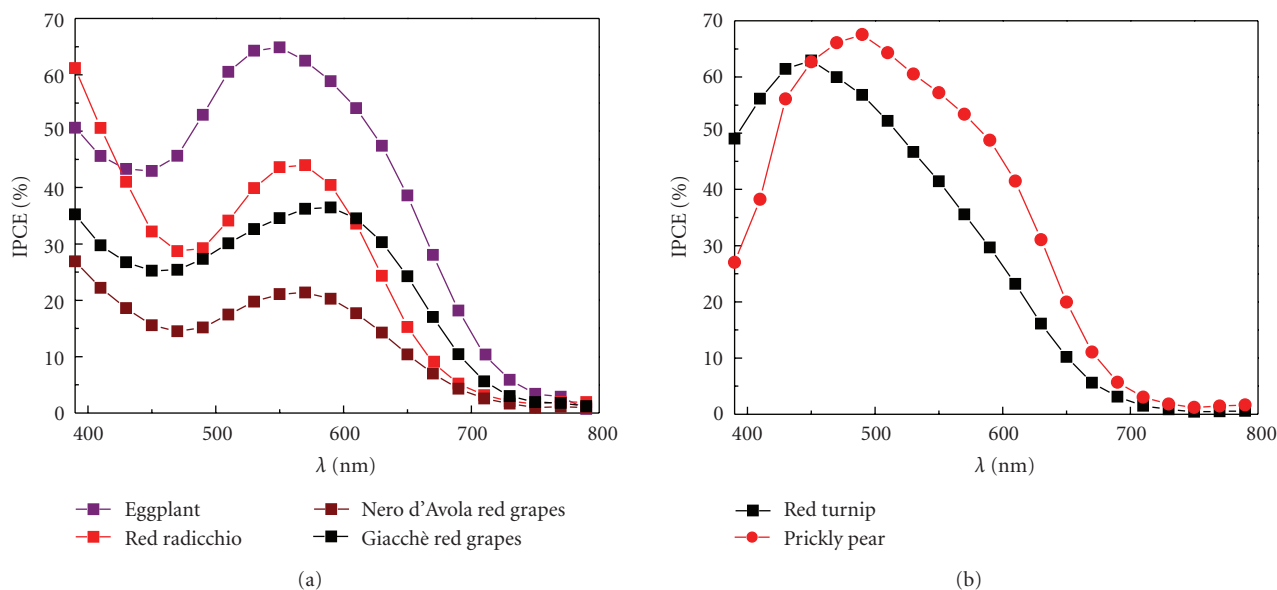
FIGURE 4: Photoaction spectra on transparent TiO$_2$ of (a) anthocyanine raw extracts from eggplant (purple), red radicchio (red), Giacchè red grapes (black), and Nero d'Avola red grapes (brown); (b) betalains from red turnip (black) and wild prickly pear (red). LiI/I$_2$ 0.5 M/0.05 M in ACN was used as a redox electrolyte.

cation recombination can also be critical compared to ruthenium sensitizers, in which the hole is confined into a metal centred d orbital relatively decoupled from the semiconductor surface. Electron recapture by smaller flat organic molecules is expected to be faster, since the hole is probably located in closer proximity to the nanoparticle surface. Indeed the spectroscopic investigation of series of cyanine dyes showed electron/hole recombination lifetimes lower than 200 ns.

3. Electron Mediators Based on Coordination Compounds

So far the I$_3^-$/I$^-$ couple has been the most efficient and commonly used redox mediator in DSSCs, due to the fast regeneration of the oxidized dye provided by I$^-$ on a nanosecond time scale [33, 34] (Figure 5). The reduction of I$_3^-$ is a complex multistep reaction involving the breaking of chemical bonds: some authors [35, 36] have studied it in great detail and suggested a first dissociation of I$_3^-$ in I$^-$ and I$_2$, a subsequent reduction of I$_2$ to I$_2^-$ followed by the rate limiting dismutation of two I$_2^-$ to give I$^-$ and I$_3^-$. The same authors suggested that the reduction of I$_2$ occurs only with adsorbed I$_2$ molecules and the overall process is further slowed down by its relatively low concentration compared to I$_3^-$ in solution; moreover it is efficiently catalyzed by the presence of Pt at the counter electrode.

The electronic recapture involving I$_3^-$ is kinetically so slow on both TiO$_2$ and FTO surfaces that, under short circuit conditions, most of electrons survive the transit through the mesoporous film and the FTO surface and appear in the external circuit. In summary, the forward electron donation by I$^-$ is a facile monoelectronic process which
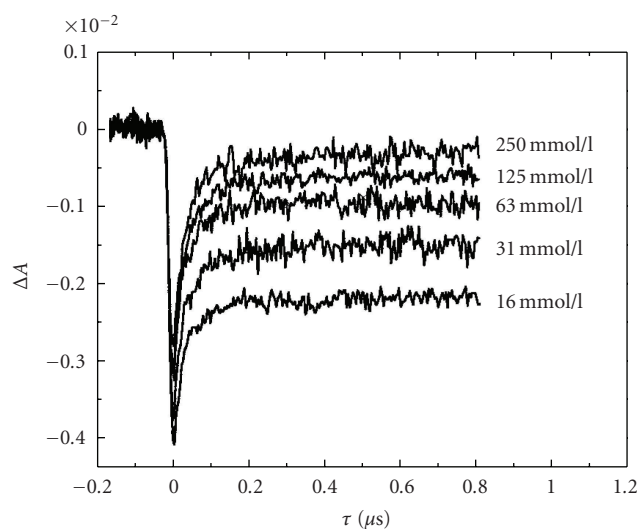

FIGURE 5: N3 recovery in presence of increasing concentration of NaI in acetonitrile.

ensures an efficient dye recovery (k_4 in Figure 1), while the reduction of I$_3^-$ appears to be largely inefficient allowing for a minimization of the interfacial back recombination (k_6 in Figure 1).

In other respects the I$_3^-$/I$^-$ redox couple is less than ideal for a number of reasons: I$_2$ in equilibrium with I$_3^-$ is volatile, complicating long-term cell sealing; I$_3^-$ is darkly colored and limits the light harvesting efficiency of the dye; DSSC cathodes require platinum coatings to effectively catalyze the I$_3^-$ reduction. Most importantly, I$_3^-$/I$^-$ is corrosive towards many highly conductive metals, posing a serious problem for the scaling up of the solar cells to large areas which
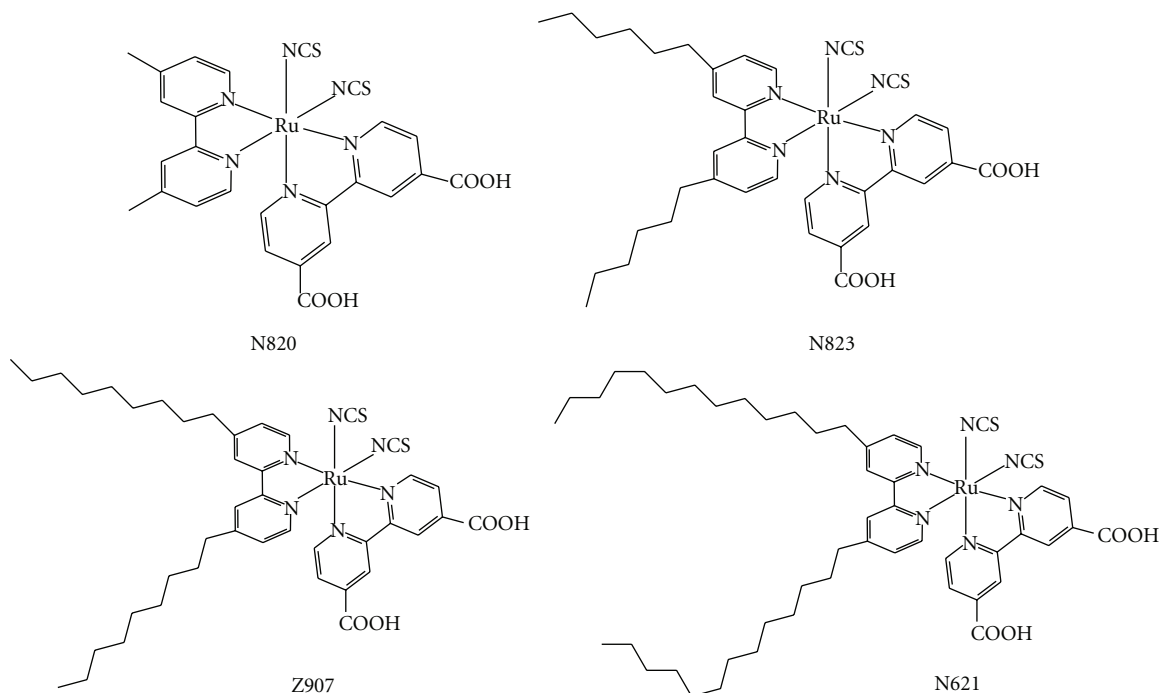
Figure 6: Heteroleptic dyes used in conjunction to cobalt electron transfer mediators.

requires the use of metallic grids deposited on FTO in order to minimize ohmic losses due to the high sheet resistance of the transparent conductive substrate. Besides these practical problems the search for new electron transfer mediators potentially capable of replacing the I_3^-/I^- couple is challenging for a number of reasons related to the strict requirements that must be fulfilled by an efficient electron mediator: it has to intercept efficiently the oxidized form of the dye, recombine slowly with photoinjected electrons on both TiO_2 and FTO substrates, and allow for an efficient mass transport in solution and into the TiO_2 mesopores. To our knowledge, there is no certain a priori indication that such requirements would be satisfied by a given chemical species on a specific substrate; however, in principle, every system characterized by a high reorganization energy associated to the electron transfer should exhibit a slow kinetics. In the following we report on the main attempts made to develop and improve new redox systems for DSSCs based on coordination compounds and on conductive polymers.

The electrochemical properties of coordination compounds can be tuned through a rational choice of the metal and an appropriate design of the coordination sphere. These features might guarantee the necessary flexibility to project an electron transfer mediator capable of meeting the kinetic requirements outlined above. In principle, to minimize recombination, kinetically slow couples have to be privileged. The relatively high concentration of electrolyte employed in photoelectrochemical cells (0.1–0.5 M in redox active species) demands for inexpensive and available metals, like the elements of the first transition row, and easily synthesizable ligands. To date, the most successful attempts have been based on octahedral cobalt(II) and tetrahedral copper(I) complexes. The Co(II)/(III) couple is usually

characterized by an high inner sphere reorganization energy associated to the electron transfer, essentially due to the involvement of a metal centred e_g redox orbital with antibonding characteristics.

One of the first reports by Graetzel and coworkers was focused on the use of a one-electron Co(II) redox mediator based on the Co(II)-bis-[2,6-bis(1′-butylbenzimidazol-2′-yl)pyridine] [37] (dbbip) complex. The Co(III)(dbbip)$_2^{3+}$/Co(II)(dbbip)$_2^{2+}$ potential was of 0.36 V versus SCE, a value comparable with that of the I_3^-/I^- couple. Used in conjunction with a compact blocking TiO_2 underlayer, whose function is devoted to the minimization of the dark current (recombination with Co(III)), Co(dbbip)$_2$ appeared to rival the I_3^-/I^- performances in terms of IPCE and global cell efficiency. Encouraging was also the weak coloration of the complex which exhibited a moderate absorption in the visible region with an extinction coefficient of the order of 10^2 mol^{-1}1 cm^{-1} at 450 nm. The best results with this type of cobalt mediators were obtained using heteroleptic complexes like Z907 and N 621 bearing long alkyl chains (Figure 6).

The use of heteroleptic dyes [38, 39] brings two main advantages: reduction of the ion pairing effect due to a smaller negative ζ potential and suppression of the electron tunnelling to Co(III) acceptors caused by the steric hindrance of the long alkyl chains, which limit the access of the cobalt complex to the exposed TiO_2 surface, thus reducing the probability of electron recapture as evident from the cell dark current measurements. For similar reasons the cografting of long alkyl chain carboxylic acids like hexadecylmalonic acid allowed for an enhancement of the photovoltaic response of cobalt-mediated cells [39]. One of the limitations of Co(II) benzimidazol complexes is related to the multistep synthetic procedure for the ligand preparation.
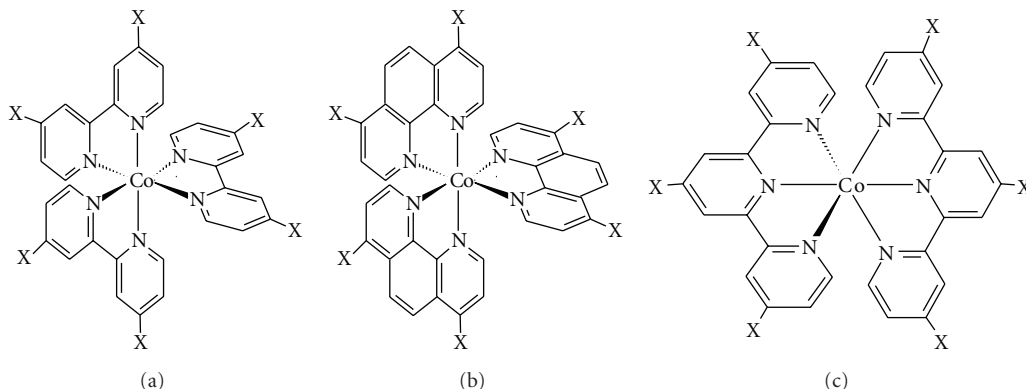
(a)   (b)   (c)

FIGURE 7: Structure of polypyridilic Co(II) complexes: (a) X = Tert-butyl (DTB), Methyl (DMB), H (bpy). (b) X = H (phen). (c) X = Tert-butyl (tTbterpy), Ethyl (tEterpy).

Almost contemporarily to the efforts made at the Swiss Federal Institute of Technology of Lausanne, it was found that particular cobalt polypyridine complexes, formed from structurally simple ligands, did function as efficient electron-transfer mediators in DSSCs [40].

The main focus of the investigation was thus to identify which structural and thermodynamic motifs generate the best mediators, allowing for the assembly of cells with the closest match to the performance of the I_3^-/I^- mediator.

The cobalt complexes reported in Figure 7 can be easily produced by mixing 1 equivalent of $[Co(H_2O)_6]^{2+}$ with 3 equivalents of a bidentate ligand or 2 equivalents of a tridentate ligand under magnetic stirring in refluxing methanol for 2 hours. Addition of ethyl ether results in the precipitation and isolation of the product which is then usually used without any further purification.

All of the complexes under consideration exhibit similar UV-Vis absorption spectra characterized by a weak absorption band centred at ca. 440–450 nm and a ligand-based π-π^* transition above 350–380 nm.

The most intense visible absorption is for $Co(tTbterpy)_3^{2+}$ with $\varepsilon_{450} = 1.4 \leftarrow 10^3\,M^{-1}\,cm^{-1}$ while the other complexes exhibit $\varepsilon_{440–450}$ values that are approximately an order of magnitude smaller. For the sake of comparison, the $\varepsilon_{440–450}$ value for I_3^- is ca. $2 \leftarrow 10^3\,M^{-1}\,cm^{-1}$; therefore, except $Co(tTbterpy)_3^{2+}$ that has a comparable absorbance, considerably less visible light is absorbed by all of the remaining cobalt complexes at similar concentrations.

Electrochemical characterization of these complexes revealed an unexpected electrode material dependence to the electron-transfer kinetics. In the case of 4-4′ substituted polypyridine Co(II) complexes, gold electrodes exhibit the most reversible and ideally shaped CVs. Glassy carbon and platinum electrodes also produce quasireversible voltam-mograms, although less reversible than gold. In general, the shapes of the quasireversible waves indicate that, in cases where the heterogeneous electron transfer is slow, the transfer coefficient, α, is considerably greater than 0.5. In other words, for equivalent overpotentials the heterogeneous reduction of the Co(III) complex is considerably faster than the corresponding oxidation of the Co(II) species. The
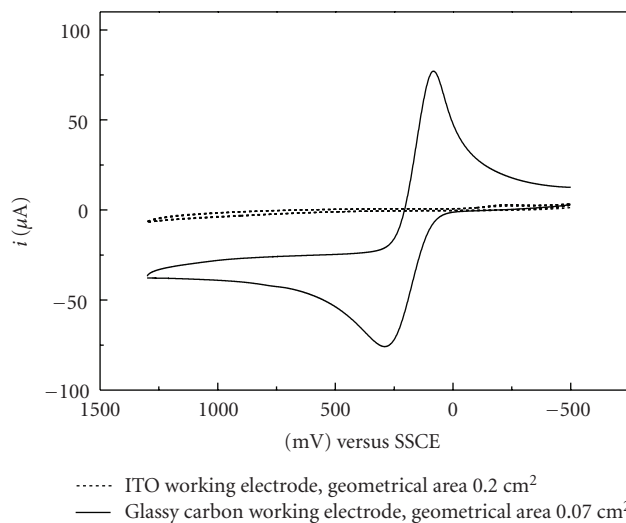

------ ITO working electrode, geometrical area 0.2 cm^2
—— Glassy carbon working electrode, geometrical area 0.07 cm^2

FIGURE 8: Cyclic voltammetry of approximately $1 \times 10^{-3}\,M$ $Co(DTB)_3^{2+}$ recorded in ACN/TBAPF$_6$ 0.1 M on GC (solid line) and on ITO (dotted line).

voltammetric results also suggest that while platinum is the cathode of choice for the I_3^-/I^- redox mediator, it should *not* be the optimal choice for cobalt complex-based mediators. Likewise, while carbon has long been considered a poor cathode for I_3^-/I^-, it should be acceptable for any of the cobalt systems considered here. It should be considered that only very recently significant results concerning alternative high-performance counter electrodes for the I_3^-/I^- couple, based on particular carbonaceous materials (nanotubes, graphene, carbon black), have been reported [41–44]. It must be noted that, among the series of Figure 7, one of the most promising cobalt complexes $(Co(DTB)_3^{2+})$ is nearly *electrochemically inactive* on FTO and ITO electrodes (Figure 8), meaning that the unwanted Co(III) to Co(II) reduction at the photoanode requires high overpotentials to be effective.

The dramatic dependence of the $Co(DTB)_3^{2+/3+}$ hetero-geneous electron transfer rate on the chemical nature of the electrode surface is most probably consequence of specific
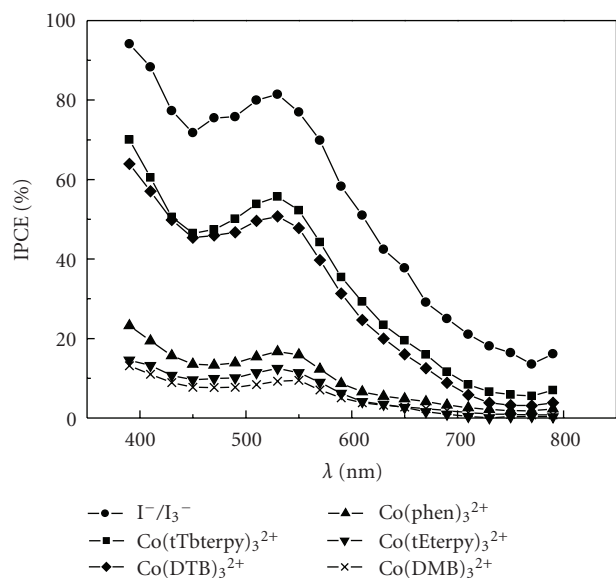
FIGURE 9: Photoaction spectra of N3 bound to nanocrystalline TiO$_2$ films in the presence of different electron mediators in MPN solutions: 0.25 M LiI/25 mM I$_2$ (circles), 0.25 M Co(tTBterpy)$_2^{2+}$/25 mM NOBF$_4$ (squares), 0.25 M Co(DTB)$_3^{2+}$/25 mM NOBF$_4$ (diamonds), 0.25 M Co(phen)$_3^{2+}$/25 mM NOBF$_4$ (triangles), 0.25 M Co(tEterpy)$_2^{2+}$/25 mM NOBF$_4$ (upside down triangles), and saturated (<0.15 M) Co(DMB)$_3^{2+}$/25 mM NOBF$_4$ (crosses). 0.25 M LiClO$_4$ was added to all solutions containing a cobalt mediator.

interactions between the surface and the electroactive species which modify the electronic coupling and/or the activation barrier for the heterogeneous electron-transfer reaction. The electrochemical behaviour on metal oxide surfaces is in this case similar to that of the I$_3^-$/I$^-$ couple for which the electron transfer from the FTO substrate to I$_3^-$ is a very slow multistep process [45].

The performances of the photoelectrochemical cells are strongly dependent on the composition of the electrolyte solution (Figure 9).

A maximum conversion efficiency of ca. 80%, in correspondence to the metal-to-ligand charge transfer absorption maximum of N3, was obtained in the presence of 0.25 M LiI/0.025 M I$_2$, whereas, with the cobalt based mediators, the best performances (IPCE ca. 50%–55%) were observed when solutions of Co(DTB)$_3^{2+/3+}$ and Co(tTBterpy)$_2^{2+/3+}$ were used. Co(phen)$_3^{2+/3+}$ Co(tEterpy)$_2^{2+/3+}$ and Co(DMB)$_3^{2+/3+}$ mediators exhibited much lower conversions, with maximum IPCE values in the range of 10%–20%.

Generally, cobalt complexes of unsubstituted and methylsubstituted bipyridine or terpyridine ligands are poor electron transfer mediators in the type of DSSCs considered herein. In contrast, if the ligand contains a tertiary butyl substituent in the para position, the resulting cobalt-based cells yield quite good IPCE. The observed substituent effect cannot be related to an electronic perturbation of the Co(II) redox orbitals and to a consequent modification of the electrochemical properties of the coordination compound, since the electron-donating effect of all simple alkyl

substituents (e.g., methyl, ethyl, *tert*-butyl, etc.) is essentially the same [46] and all of the complexes of a given ligand-type (i.e., bipyridine, phenanthroline, or terpyridine) were expected and found to have very similar $E_{1/2}$ (100–200 mV versus SCE) values for the relevant Co(II/III) couple.

Nanosecond transient absorption experiments allowed for the rationalization of the lower efficiency of the Co-based couples with respect to I$_3^-$/I$^-$ and for the clarification of their structure-dependent performance. Figure 10(a) shows the decay of the photogenerated N3 dye cation, observed at 480 nm in the presence of Co(DTB)$_3^{2+}$ 0.1 M and TBAI 0.1 M: in both cases a $\tau_{2/3}$ of about 0.35 μs indicates that dye regeneration by I$^-$ and by Co(II) occurs at a very similar rate.

Upon Li$^+$ addition (Figure 10(b)) an increased reduction rate by iodide is observed ($\tau_{2/3}$ = 0.12 μs), whereas regeneration of the oxidized dye by Co(II) is substantially unchanged. Indeed, TiO$_2$ surface adsorption/intercalation by Li$^+$ creates a positive polarization which attracts a surface excess of iodide in close proximity of the dye sites, allowing for a faster interception of the oxidized sensitizer. The same effect is obviously absent in the case of positively charged Co(II) complexes which do not experience any attraction with a positively polarized photoelectrode.

Recombination of injected electrons with the oxidized mediator could be particularly serious in the case of Co(II)/(III) electron transfer mediators in which the outer sphere monoelectronic Co(III) reduction at the photoanode could be considerably more efficient than the multistep I$_3^-$ reduction.

The process can be probed by means of transient spectroscopy following the time evolution of dye-cation bleaching. Reduction of the oxidized mediator by photoinjected electrons results in a slowing down of dye absorption recovery.

From Figure 11(a) it is evident that I$_3^-$ gives rise to the smallest increase in $\tau_{2/3}$ of the oxidized sensitizer, meaning that the CB electron interception has the lowest efficiency within the series of mediators explored so far. On the other hand Co(III) complexes produce a consistent increase in the recovery time of N3$^+$ (Figures 10(a) and 10(b)), showing that the back electron transfer from TiO$_2$ (or from the exposed SnO$_2$ back contact) is more efficient than in the case of I$_3^-$. It is also evident that Co(bpy)$_3^{3+}$ is by far more effective than Co(DTB)$_3^{3+}$ in recombining with photoinjected electrons. This behaviour is a convincing evidence that Co(II)/(III) mediators need bulky substituents to minimize the undesired recombination with CB electrons. On the other hand, ligand-mediated recombination can be safely excluded, since their reduction potential is generally too negative (about −1 V versus SCE) to be accessible for TiO$_2$ conduction band electrons.

In the effort of improving the performance of such mediators the possibility of using kinetically fast couples in conjunction with the best Co(II) mediators has been explored [47].

Kinetically fast couples efficiently reduce the oxidized dye, but due to the fast recombination with injected electrons, are totally unsuccessful as mediators in DSSCs. However, when mixed with an excess of cobalt mediator, if
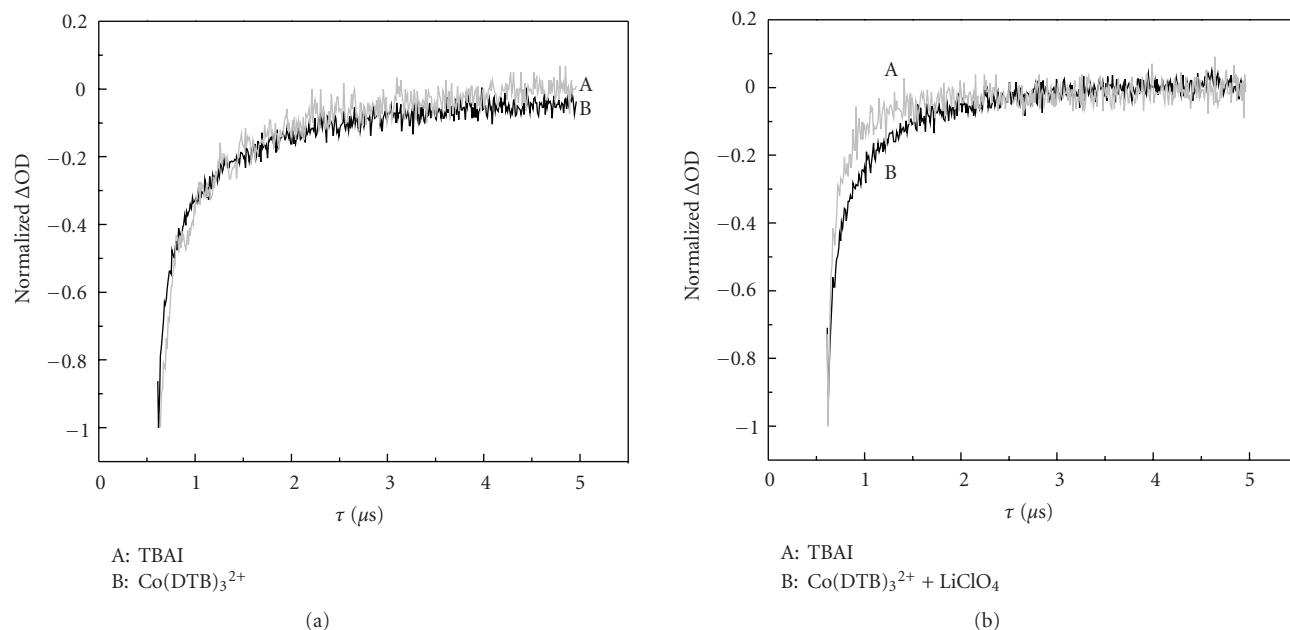
A: TBAI
B: Co(DTB)$_3$$^{2+}$

(a)

A: TBAI
B: Co(DTB)$_3$$^{2+}$ + LiClO$_4$

(b)

FIGURE 10: 480 nm Ru(III)(H$_2$DCB)$_2$(NCS)$_2$$^+$ recovery in the presence of (a) Tetrabutyl-ammonium iodide (A) and Co(DTB)$_3$$^{2+}$ (B) 0.1 M; (b) Tetrabutyl-ammonium iodide (A) and Co(DTB)$_3$$^{2+}$ (B) 0.1 M + LiClO$_4$ 0.1 M. Pulse energy $\approx$ 1 mJ/cm^2.

A: Neat solvent
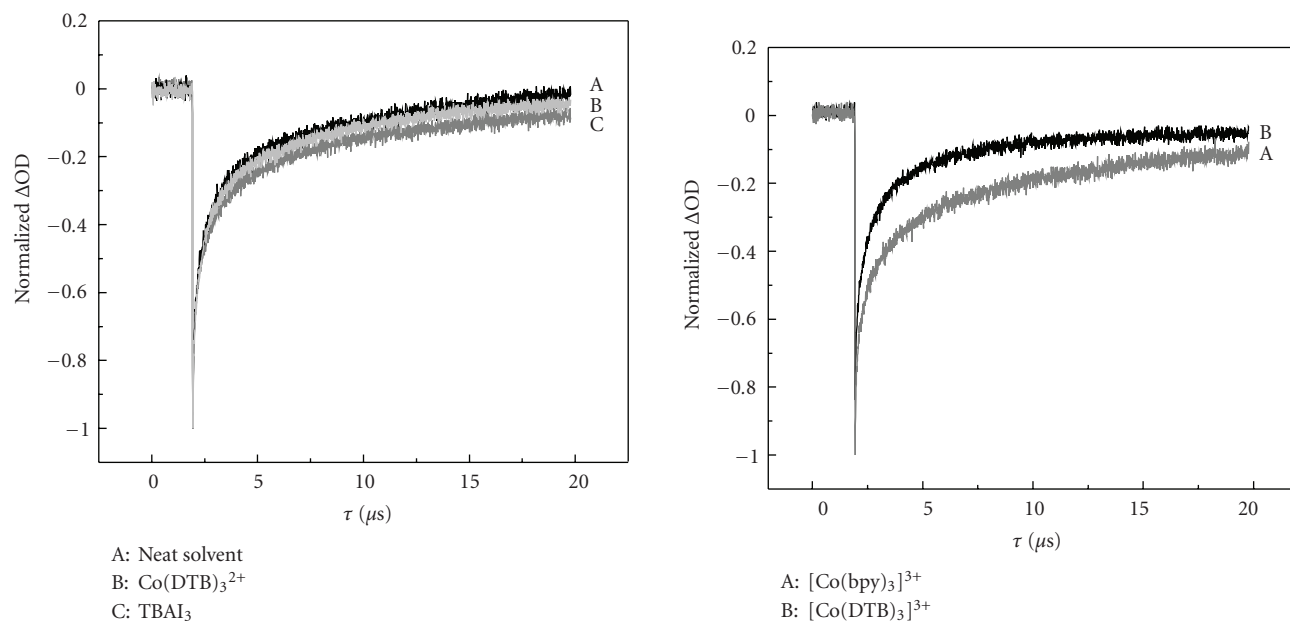B: Co(DTB)$_3$$^{2+}$
C: TBAI$_3$

A: [Co(bpy)$_3$]$^{3+}$
B: [Co(DTB)$_3$]$^{3+}$

FIGURE 11: 480 nm Ru(III)(H$_2$DCB)$_2$(NCS)$_2$$^+$ recovery in the presence of (a) neat solvent (γ butyrolactone) (A), 0.1 M Co(DTB)$_3$$^{3+}$ (C), and Tetrabutyl-ammonium triiodide (B); (b) Co(DTB)$_3$$^{3+}$ (B) and Co(bpy)$_3$$^{3+}$ (A). Pulse energy $\approx$ 1 mJ/cm^2.

their redox potential is appropriate (i.e., more positive than the Co(III)/(II) couple), a cascade of electron transfer events allows to confine the hole on Co(III) (Figure 12) which, by virtue of its very slow heterogeneous electron transfer on semiconductor oxides, gives rise to a very inefficient electron recapture. As a consequence, the large majority of Co(III) created in the second electron transfer step is free to diffuse to the counter electrode of the cell, whereupon it is reduced.

The use of a long alkyl chain dyes like Z907, for example, is beneficial to the system allowing to further reduce back recombination enhancing the electron collection efficiency.

Phenothiazine (PTZ) and ferrocene (Fc), both having a small reorganization energy associated to the electron transfer, are the first comediators that have been considered. Each has a potential which falls between that of the Co(DTB)$_3$$^{3+/2+}$ (0.22 V versus SCE) and of the
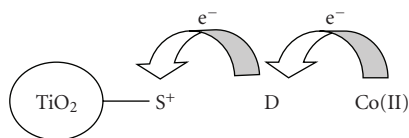
FIGURE 12: Sequence of electron transfer events involving the oxidized dye (S+) the comediator (D) and the cobalt complex (Co(II)).
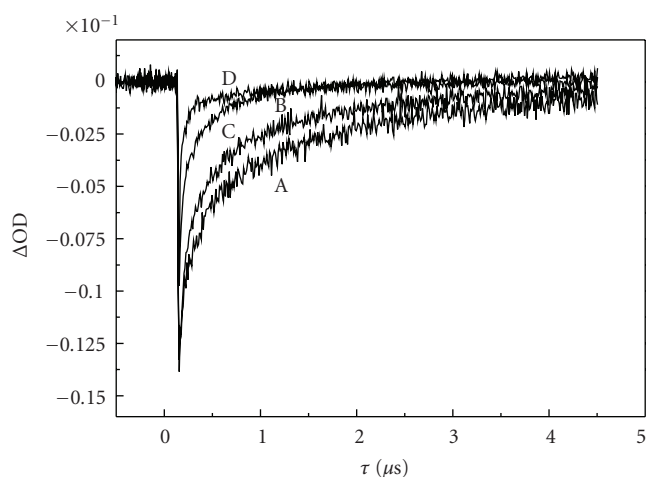

FIGURE 13: Decay kinetic of photooxidized Z907 adsorbed on TiO$_2$ in the presence of various electron mediators: (A) no mediator; (B) 0.1 M Co(DTB)$_3^{2+}$; (C) 0.1 M PTZ; (D) 0.1 M Fc. Differential absorbance changes are measured at 480 nm. Pulse energy: 5 mJ/cm^2.

dye [Ru(H$_2$DCB)(dnbpy)(NCS)2]$^{+/0}$ (0.75 V versus SCE). Because of the facile electron transfer the photooxidized dye would be predominantly reduced by the comediator. Its oxidized form (PTZ$^+$ and Fc$^+$) can be then rapidly intercepted by Co(II), preventing the direct charge recombination between the oxidized comediator and the electrons in the TiO$_2$. Nanosecond transient absorption measurements confirmed a faster dye regeneration by both PTZ and Fc relative to Co(DTB)$_3^{2+}$, despite their higher redox potential (Figure 13).

The best results were observed using a comediator/Co(II) ratio of 1 : 2 with 0.15 M Co(DTB)$_3^{2+}$ in acetonitrile. Addition of 0.5 M Li$^+$ and 0.1 M ter-butyl-pyridine generally improved the open circuit photovoltage. In the presence of the PTZ/Co(II) mixture cell IPCE% reached more than 80% (Figure 14(b)), a value well comparable to the best I$_3^-$/I$^-$ cells. Under white light irradiation J_{sc} was also comparable, with the advantage of a better fill factor and higher Voc for the cobalt-based cell (Figure 14(a)).

In general the Fc/Co(II) mixture gave poorer overall photovoltaic performances than the equivalent PTZ/Co(II) system, notably a poorer Voc and fill factor. Since ferrocene was found to be faster in dye regeneration, an explanation can lie in a less efficient interception of Fc$^+$ by Co(II) centres,

resulting in a larger steady state concentration of Fe(III) which undergoes recombination on the TiO$_2$ surface. Indeed, chronocoulometry and cyclic voltammety experiments at FTO electrodes allowed to verify that PTZ$^+$ was from 1.5 to 2 times more effective than Fc$^+$ in the oxidation of Co(II), thus having a smaller probability of recombining with photoinjected electrons.

An analogous behaviour extends to other species having small reorganization energies and appropriate potentials such as the iron(II) complexes Fe(DMB)$_3^{2+}$ and Fe(DTB)$_3^{2+}$ ($E_{1/2} \approx 0.95$ V versus SCE). When used in the presence of an excess of Co(DTB)$_3^{2+}$ and in conjunction with suitable sentizers like the heteroleptic dye Ru(dnbpy)(H$_2$DCB)$_2^{2+}$ ($E_{1/2} = 1.25$ V versus SCE) (Figure 15) the Fe(II) comediators clearly enhance the performance of the Co(DTB)$_3^{2+}$ and outperform the I$_3^-$/I$^-$ redox couple, at least in terms of IPCE, with maximum values close to 85%.

Interestingly, the polypyridine Fe(II)/Co(II) mediator mixtures were rather insensitive to variations of the Fe(II) to Co(II) concentration ratio ranging from 0.1 to 0.5, with the optimum at 0.1. For higher Fe(II)/Co(II) ratios the cell performance dropped, ostensibly due to the formation of an excess of Fe(III) which was no longer effectively intercepted by Co(II) and recombined on the TiO$_2$ surface. In the case of electron mediator mixtures characterized by the presence of a kinetically fast couple, the decrease in ζ potential and the blocking effect obtained by using heteroleptic dyes with hindering chains is more than ever important for controlling electron recapture: meaningfully, the performances of the Fe(II)/Co(II) mixtures used in conjunction with the homoleptic Ru(H$_2$DCB)$_3^{2+}$ (where DCB is the 4,4′dicarboxylic acid 2,2′ bipyridine) were rather poor, not exceeding a maximum IPCE% of 30%, whereas the I$_3^-$/I$^-$ couple produced almost identical conversions (ca. 40%) to those reported with the heteroleptic Ru(dnbpy)(H$_2$DCB)$_2^{2+}$.

The Fe(II)/Co(II) mediators displayed an interesting behaviour in conjunction with bisterpyridine complexes (formula in Figure 16) which, when used with the I$^-$/I$_2$ couple, have been known to be rather poor sensitizers. The IPCE% improved from the 20% obtained in the presence of LiI/I$_2$ to 30% with Co(DTB)$_3^{2+}$ alone, to more than 60% using the Fe(DMB)$_3^{2+}$/Co(DTB)$_3^{2+}$ system (Figure 16).

Spectroscopic investigation evidenced that this enhanced performance could not be explained by an improved dye regeneration by the cobalt-based mediators: despite giving rise to an efficient dye recovery (14 ns and 9 ns for the Co(II) and the Fe(II)/Co(II) mixture, resp.) these metal-based mediators were still slower than iodide, which produced an instrument response-limited ($\leq$7 ns) Ru(II) regeneration. Further investigations indicated, however, that the oxidized form of the iodide-based mediator, namely, triiodide, was consistently more effective than Co(III) in capturing conduction band electrons, producing a notable increase in the Ru(III) lifetime (Figure 17).

Thus the relatively low IPCE% observed with I$_3^-$/I$^-$ appeared to be essentially determined by an efficient electron recombination with triiodide. This phenomenon, surprising at first, could be caused by a number of factors ranging
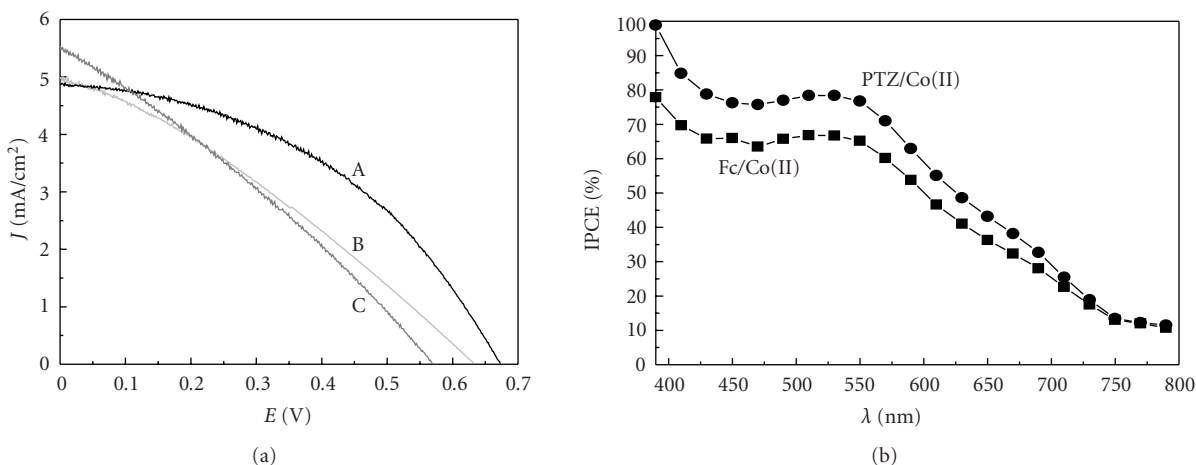
(a)

(b)

FIGURE 14: (a) J-V curves obtained in the presence of Co(II)/PTZ (A), I_3^-/I^- (B), and Co(II)/Fc (C) in methoxypropionitrile. (b) Photoaction spectra. Incident irradiance $\approx 0.1 \, W/cm^2$.
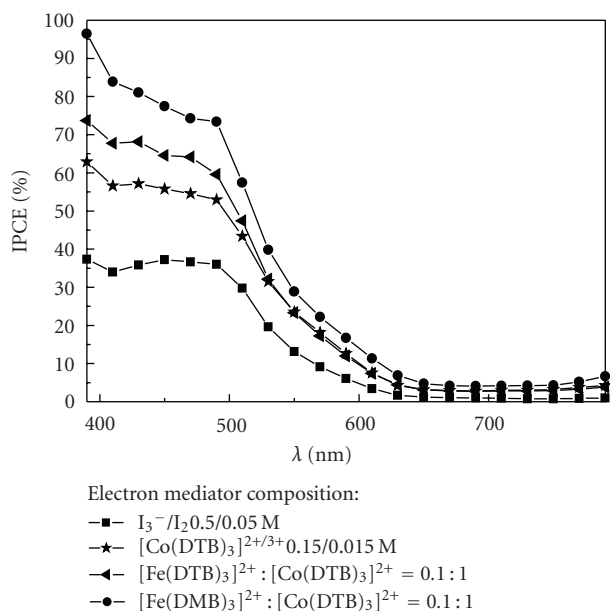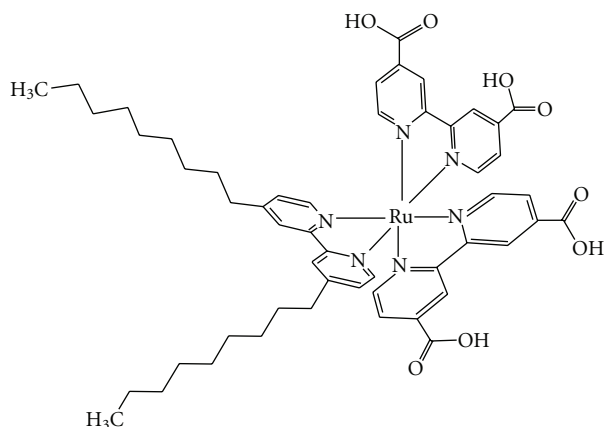

Electron mediator composition:
- —■— $I_3^-/I_2 \, 0.5/0.05 \, M$
- —★— $[Co(DTB)_3]^{2+/3+} \, 0.15/0.015 \, M$
- —◀— $[Fe(DTB)_3]^{2+} : [Co(DTB)_3]^{2+} = 0.1 : 1$
- —●— $[Fe(DMB)_3]^{2+} : [Co(DTB)_3]^{2+} = 0.1 : 1$

FIGURE 15: IPCE spectra of $Ru(dnbpy) \, (H_2DCB)_2^{2+}$ obtained in the presence different electron transfer mediators.

from an insufficient TiO_2 surface passivation by the dye against the small I_3^- ions, to specific interactions between the complex and I_3^- which lead to iodine association via the sulphur atom of the thiophene ring and to the induction of a positive surface charge upon adsorption of the cationic Ru(II) dye possessing only one carboxylic function. The positively charged surface might attract I_3^- favouring recombination and, on the contrary, might repel Co(III), ultimately reducing the probability of electron recapture in the latter case. Thus it seems that, depending on their structure and charge, each dye interacts specifically with different electron mediators in ways that are worth to be studied, since they may lead to both fundamental and practical advances in DSSC design in the future.

4. Solid State Conductive Polymers

Conductive polymers based on polythiophenes and polypyrroles could be interesting candidates for replacing the liquid electrolyte in DSSC, due to their low cost, thermal stability, and good conductivity [48]. Thanks to these properties, these systems have already found application in the OLED technology as charge transporting matrices. PEDOP (poly-ethylene-dioxy-pyrrole) can be deposited on a sensitized TiO_2 photoanode via a photoassisted electropolymerization [49] initiated by the purpose built ruthenium complex $[Ru(H_2DCB)(pyrr-bpy)_2]^{2+}$ [50] (Figure 18): the oxidized dye, $[Ru^{III}(H_2DCB)(pyrr-bpy)_2]^{3+}$, created after the charge injection into TiO_2, is a sufficiently
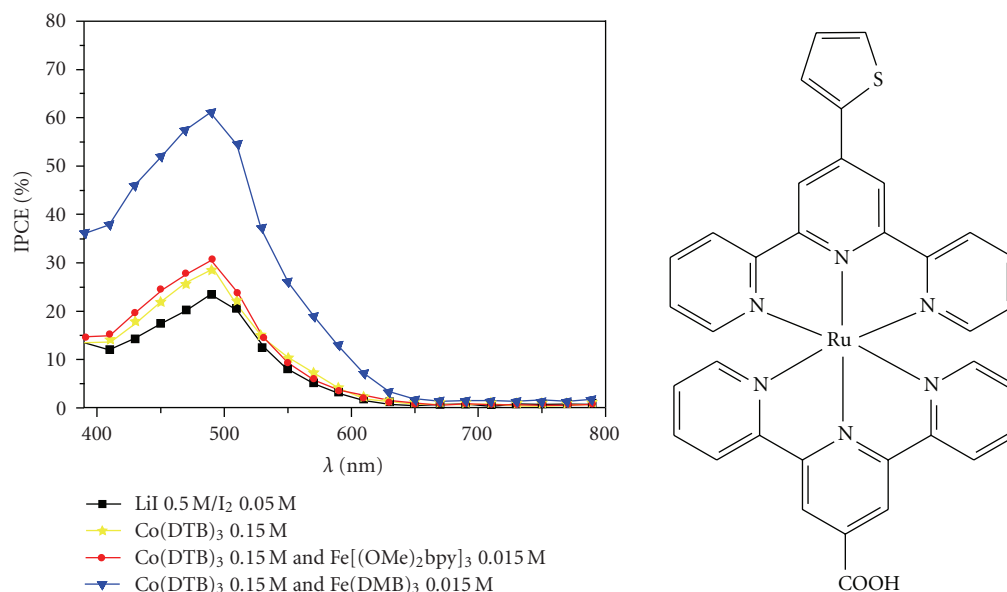
FIGURE 16: IPCE spectra in the presence of various electron mediators obtained by using the $[Ru(II)(terpy)(Thpterpy)]^{2+}$ dye as a TiO_2 photosensitizer. Thpterpy stands for the 4′-thiophene terpyridine.
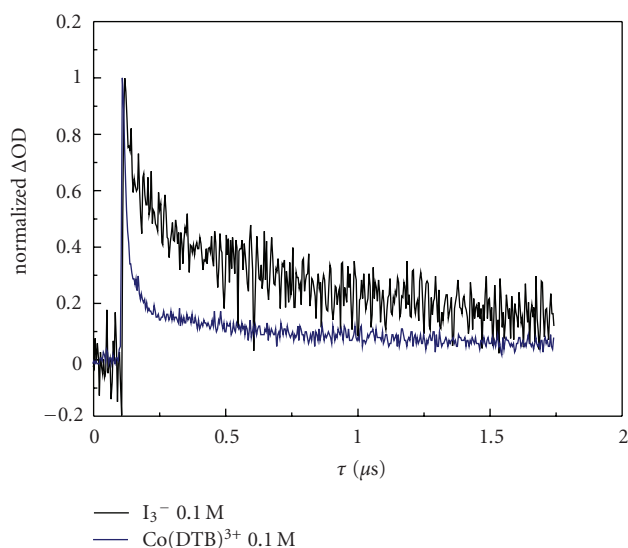

FIGURE 17: Differential absorption decays for Ru(III) recovery observed at 750 nm in the presence of equimolar amounts of I_3^- and Co(III) in acetonitrile $+0.5\,M$ Li^+. Excitation energy density $\approx 1\,mJ/cm^2/pulse$.

strong oxidizer, with a potential of 1.19 V/SCE, to oxidize EDOP monomers and induce their cationic polymerization, leading to the growth of polymeric chains chemically attached to the dye with a possible advantage in terms of electronic coupling and charge transfer rate between electron donor (PEDOP) and acceptor (oxidized dye).

A typical solar cell assembled according to this approach is comprised of a photoanode, functionalized with PEDOP, firmly clamped together with a gold-coated FTO counter electrode. A 0.3 M $LiClO_4$ solution in γ-butyrolactone is eventually drawn inside the cell by capillarity.

Our results on these types of cells showed very low efficiencies mostly due to small J_{sc} ($<200\,\mu A$) and poor fill factors (≤ 0.31). The J-V characteristics of solid state PEDOP cells (Figure 19) indicate a strong recombination and a high serial resistance.

Dark current measurements performed under direct voltage bias showed a marked increase in recombination efficiency as the bias approached -0.4 V, near the onset of PEDOP reduction, suggesting that higher lying states of TiO_2 were filled promoting recombination with PEDOP holes.

While the dark current suggested a possible photocurrent loss mechanism through PEDOP reduction, a relevant recombination with the oxidized dye could not be ruled out. Dark current simply could not provide information on the latter process since, in the dark, after equilibrium was attained, no oxidized Ru(III) centres should be present at the TiO_2/Dye/polymer interface.

Indications of efficient recombination were also gained from cell photocurrent transients under short circuit conditions, showing cathodic spikes due to recombination of photoinjected electrons with PEDOP holes and oxidized Ru(III) centres.

The cathodic current dropped to zero on a very short time scale suggesting that recombination was kinetically fast, at least for the time scale (0.1 s sampling time) of the experiment. Passivation of the TiO_2 surface via the application of a nanometric insulating Al_2O_3 overlayer [51] was instrumental in reducing the electronic recapture, allowing for an IPCE% doubling (from 3% to 6%) (Figure 20). Cell Jsc and Voc measured under 0.05 W/cm^2 white light irradiation were also significantly improved (from 50 to 100 $\mu A/cm^2$ and from 0.4 to 0.7 V, resp.).

Pyrr-bpy =

H_2DCB =
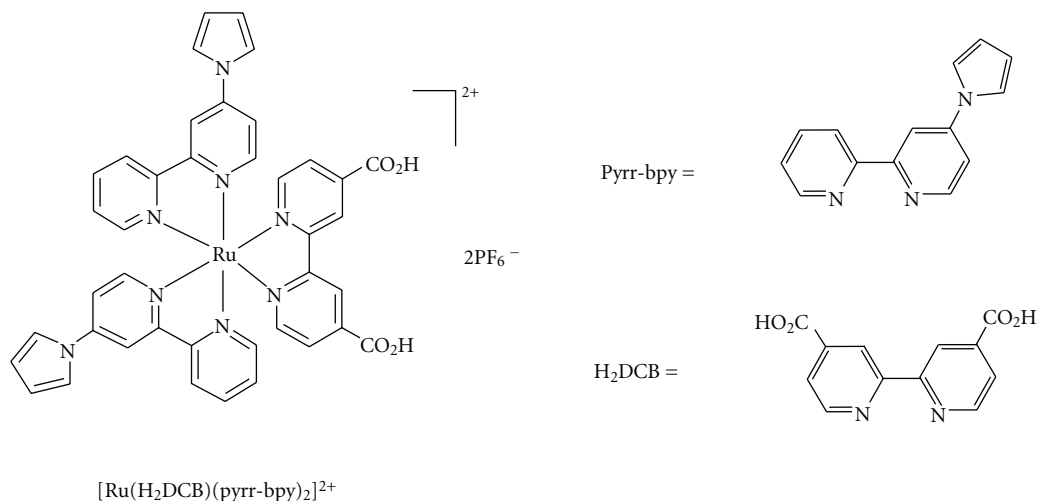
$[Ru(H_2DCB)(pyrr-bpy)_2]^{2+}$

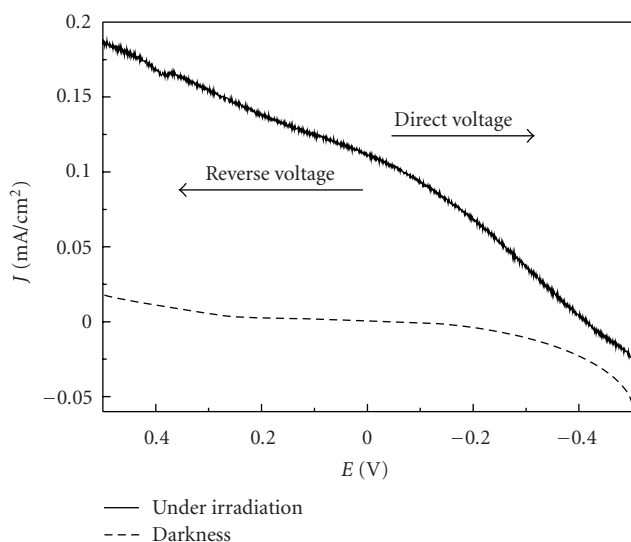FIGURE 18: Ru(II) complex uses for in situ photoassisted PEDOP growth.

FIGURE 19: J-V characteristic obtained on PEDOP-based DSSC in the presence of Li$^+$ 0.3 M. 10 seconds polymerization time.

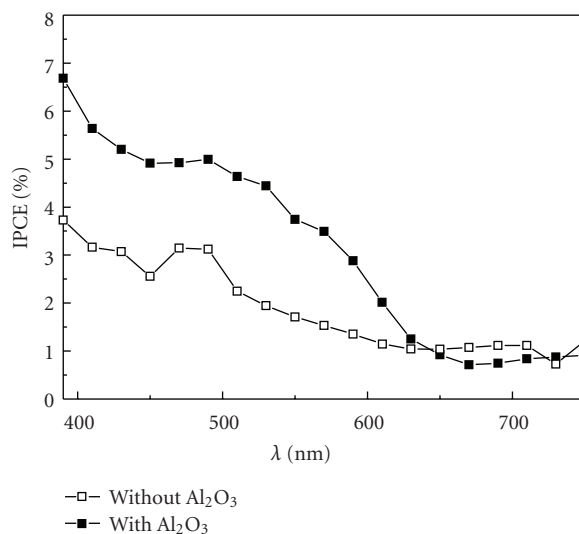FIGURE 20: Photoaction spectra of a TiO$_2$/Dye/PEDOP/Au cell (white squares) compared to a TiO$_2$/Al$_2$O$_3$/Dye/PEDOP/Au system (black squares).

Besides strong back recombination and despite the intimate contact between the dye and the hole transporting layer, the low efficiencies could also be explained by a nonoptimal hole injection into the PEDOP matrix, as evidenced by the slow oxidized dye recovery observed in transient absorbance experiments at 450 nm.

A better photovoltaic response has been recently obtained by using the excellent properties of PEDOT as a hole transporting material. As previously described, PEDOT can be in situ photo-electropolymerized from bis-EDOT monomers by exploiting the oxidizing power of a dye like Z907 [52]. The hydrophobic properties of Z907 allow for a good affinity for the scarcely polar polymeric matrix, ensuring a good electrical contact between the p-type material and the dye. The presence of a coadsorbate like deoxycholic acid (DCA) in an optimal 2 : 1 ratio with respect to the dye enhanced the global photovoltaic response by reducing dye aggregates. This function seems to be particularly relevant for polymer mediated DSSC, since aggregated dye clusters reduce the number of available polymer growth sites and leave less effective space for polymerization initiation and propagation. In order to optimize the contact between the hole transporting layer and the counter electrode, a PEDOT-functionalized FTO was used as the cathode and, to achieve optimal performances, a drop of BMImTFSI (1-butyl-3methylimidazolium bis(trifluoromethanesulfonyl)imide) containing 0.2 M LiTFSI and 0.2 M Tbpy was cast onto the TiO$_2$/dye/PEDOP junction. The ionic liquid may improve the charge transporting capabilities of the heterointerface
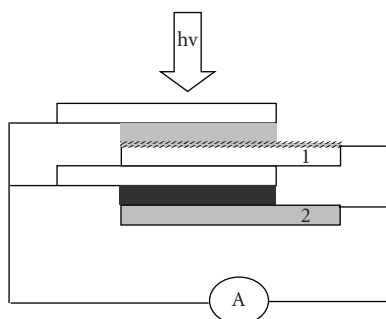
FIGURE 21: In parallel connected stacked cell based on the Co(II)/(III) couple. 1 is a transparent FTO cathode modified via chemisorption of an electroactive molecule. 2 is a conventional gold cathode. The red and the blue dyes, absorbing in complementary spectral regions, result in a panchromatic sensitization.

FIGURE 22: CV on gold (A), FTO (B), ITO (C), and osmium modified FTO (D) and ITO (E) working electrodes in the presence of ca. 0.1 mM Co(DTB)$_3$ClO$_4$. Potential referred to ferrocene.

through screening of space charge effects, lithium cations assist electron injection and percolation through the n-type semiconductor, and, as usual, tbpy increases the open circuit photovoltage via suppression of the back recombination. With such a treatment FTO/TiO$_2$/dye/PEDOT-PEDOT/FTO sandwich cells afforded efficiencies of the order of 2.6%, one of the highest results so far recorded with solid state DSSCs based on hole conducting polymers.

5. Catalytic Materials for Cathodes of DSSCs

A kinetically fast reduction of the oxidized redox mediator at the cathodic surface of the cell is required to maintain a sufficiently high concentration of electron donor thus ensuring an efficient dye regeneration. With the I$_3^-$/I$^-$ couple the use of a catalytic platinum coating is almost mandatory to achieve a satisfactory electrochemical kinetics, but the use of redox mediators alternative to the I$_3^-$/I$^-$ couple opens the way to the search for new, less expensive, more flexible, and available catalytic materials and to their application in new cell configurations. Many electrode materials (carbon, gold, platinum) function adequately in the case of Co(II)/(III) mediators but are generally opaque. In contrast, optically transparent conductive oxides (TCOs) are very poor cathodes for the Co(DTB)$_3^{2+/3+}$ couple, unless they are chemically modified by surface chemisorption of certain metal complexes. This allows to obtain optically transparent cathodes with a good electrochemical response which can be employed to build stacked cells either serially or in parallel (Figure 21) connected in which, for example, two spectrally complementary dye can work in their optimal absorption region, improving the spectral responsivity of the modules.

In a first study [53] it was demonstrated that ITO and FTO electrodes modified by irreversibly adsorbing a monolayer of Fe(H$_2$DCB)$_3^{2+}$ electrocatalyze efficiently the Co(DTB)$_3^{2+}$ oxidation via an EC′ mechanism. However, while electrogenerated Fe(III) has an ample driving force for oxidizing Co(II), Fe(II) is a thermodynamically too weak reductant for catalyzing Co(III) reduction, and the
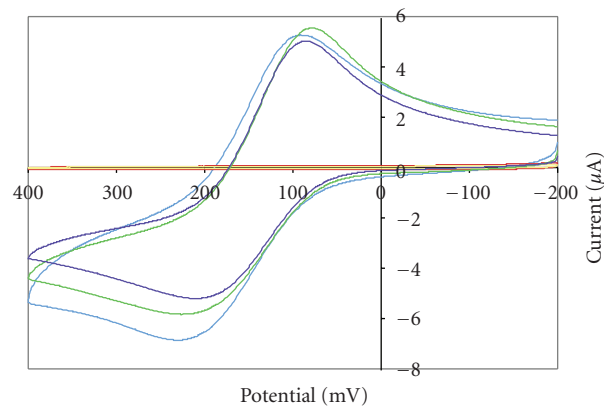
Fe(II)/(III) couple is of no value for building transparent cathodes.

Nevertheless it was found that the electrocatalysis of the Co(II)/(III) redox chemistry promoted by surface bound electroactive species is a relatively general phenomenon and a number of molecular species with appropriate potential can promote the desired catalytic effect. For example, the osmium complex Os(H$_2$DCB)$_2$Cl$_2$ can be strongly adsorbed on FTO and, with its potential (-310 mV versus Ferrocene) slightly negative of the Co(II)/(III) couple, proved to efficiently catalyze both the oxidation and reduction of Co(DTB)$_3^{2+/3+}$. Indeed, the cyclic voltammetry of Co(II)/(III) (Figure 22) recorded at osmium-modified electrodes showed well-defined quasireversible waves ($\Delta Ep \approx 140$ mV), nearly identical to those obtained on gold, whereas on the unmodified FTO or ITO it was almost impossible to observe the analogous charge transfer process. Cyclic voltammetry results were substantially confirmed by thin layer photoelectrochemical experiments which demonstrated that the osmium-modified transparent cathodes gave rise to a very small overpotential (ca. 12 mV under cell short circuit conditions) for Co(III) reduction, indicative of a facile heterogeneous electron transfer [54].

The stacked cell configuration, employing N3 and a red absorbing cyanine dye which absorbs photons in a region where N3 does not, showed a J_{sc} improvement of about 15% over a single N3 cell. It must be considered that the blue dye is relatively inefficient, generating very modest IPCE% (ca. 5%–8%) due to less than ideal redox properties and electronic coupling with the TiO$_2$. Nevertheless the results confirmed the principle and with a better performing dye substantial performance improvements are expected.

Conductive polymers like PEDOP and PEDOT were also found effective in promoting the Co(II)/(III) electrochemical response. Both PEDOP and PEDOT can be electrodeposited on a transparent conductive substrate by an anodic potentiostatic (ca. +1.3 V versus SCE) or potentiodynamic electrolysis of the appropriate precursor solution in the presence of a perchlorate containing supporting electrolyte. Co(II)/(III)
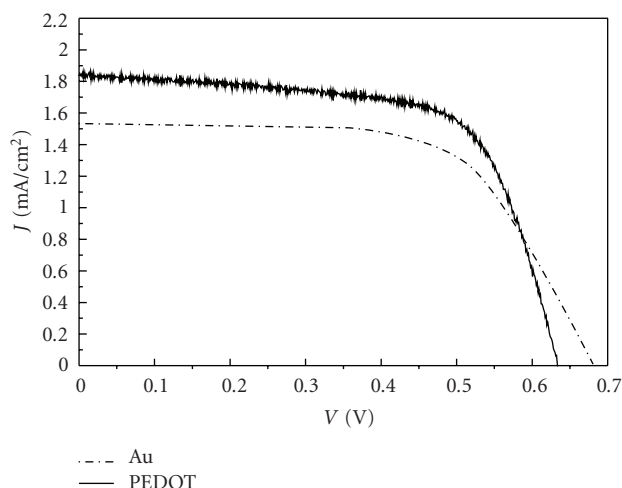
FIGURE 23: J-V curves of Co(II)/(III)-mediated cell employing a gold (dashed line) and a PEDOT counter electrode (solid line). Electrolyte composition is 0.15 M Co(II)/0.5 M Li$^+$/0.1 M Tbpy in acetonitrile. Cell is equipped with a 120 μm spacer. Photosensitizer Z907.

appeared to have a clearly diffusion-limited electrochemical behaviour on both PEDOP- and PEDOT- functionalized cathodes. PEDOT gave rise to a more ideal behaviour associated to a smaller separation of the catalytic waves, with a peak separation of the order of 200 mV, substantially independent from Co(II) concentration, the slight peak shift at higher cobalt concentration being essentially determined by uncompensated cell resistance.

The electrodeposition offers the advantage of a fine control of the thickness of the catalytic layer, thus optimizing the electroactive area and the transparency of the cathode. A cathode which possesses both a remarkable catalytic activity and a partially porous structure with a large active area is important for limiting the concentration overpotential which may develop at the counter electrode of the cell under strong illumination, allowing for the consequent reduction of the photocell series resistance. An improvement in cell fill factor and global efficiency is therefore expected and found (Figure 23).

6. Conclusions

DSSCs are photoelectrochemical solar devices, currently subject of intense research in the framework of renewable energies as a low-cost photovoltaic device.

Researches on dye sensitizers are mainly focused on transition metal complexes, but a considerable amount of work is now directed towards the optimization of organic sensitizers and of natural sensitizers extracted from fruits.

Concerning the electron mediators, iodide/iodine has been so far the most efficient and commonly used redox system, due to the fact that I$^-$ allows for a fast regeneration of the oxidized dye. The use of alternative redox couples as electron mediators has been addressed, so far, by a limited number of research groups but the results are promising.

To date, the most successful attempts have been based on octahedral cobalt(II) complexes and the best results obtained in combination with specific heteroleptic complexes. The development of efficient and noncorrosive electron mediators is considered of particular relevance since it may allow building large area modules where the different components are in parallel interconnected, increasing the single module short circuit photocurrent and allowing for a more flexible solar panel production.

The search for suitable solid materials that can replace the liquid electrolyte is an additional interesting and active area of research. Organic hole conductors like conductive polymers based on polythiophenes and polypyrroles have demonstrated some promise for application in dye-sensitized solar cells. In particular it has been reported that the presence of ionic liquids may improve the charge transporting capabilities of the heterointerface through screening of space charge effects.

Some efforts towards the modification of the counter electrode with inexpensive and transparent conductive materials have been discussed. In these studies it has been found that osmium complexes as well as electrodeposited conductive polymers like PEDOP an PEDOT are effective in promoting the electrochemical response of Co(II) electron mediators.

Acknowledgment

References

[1] R. Memming, "Electron transfer processs with excited molecules at semiconductor electrodes," *Progress in Surface Science*, vol. 17, no. 1, pp. 7–73, 1984.

[2] B. O'Regan and M. Grätzel, "A low-cost, high-efficiency solar cell based on dye-sensitized colloidal TiO$_2$ films," *Nature*, vol. 353, no. 6346, pp. 737–740, 1991.

[3] M. Grätzel, "Solar energy conversion by dye-sensitized photovoltaic cells," *Inorganic Chemistry*, vol. 44, no. 20, pp. 6841–6851, 2005.

[4] M. K. Nazeeruddin, P. Péchy, T. Renouard, et al., "Engineering of efficient panchromatic sensitizers for nanocrystalline TiO$_2$-based solar cells," *Journal of the American Chemical Society*, vol. 123, no. 8, pp. 1613–1624, 2001.

[5] C. Bauer, G. Boschloo, E. Mukhtar, and A. Hagfeldt, "Ultrafast studies of electron injection in Ru dye sensitized SnO$_2$ nanocrystalline thin film," *International Journal of Photoenergy*, vol. 4, no. 1, pp. 17–20, 2002.

[6] Y. Fukai, Y. Kondo, S. Mori, and E. Suzuki, "Highly efficient dye-sensitized SnO$_2$ solar cells having sufficient electron diffusion length," *Electrochemistry Communications*, vol. 9, no. 7, pp. 1439–1443, 2007.

[7] M. Quintana, T. Edvinsson, A. Hagfeldt, and G. Boschloo, "Comparison of dye-sensitized ZnO and TiO$_2$ solar cells: studies of charge transport and carrier lifetime," *Journal of Physical Chemistry C*, vol. 111, no. 2, pp. 1035–1041, 2007.

[8] M. Saito and S. Fujihara, "Large photocurrent generation in dye-sensitized ZnO solar cells," *Energy & Environmental Science*, vol. 1, pp. 280–283, 2008.

[9] K. Sayama, H. Sugihara, and H. Arakawa, "Photoelectrochemical properties of a porous Nb_2O_5 electrode sensitized by a ruthenium dye," *Chemistry of Materials*, vol. 10, no. 12, pp. 3825–3832, 1998.

[10] A. Kay and M. Graetzel, "Artificial photosynthesis. 1. Photosensitization of TiO_2 solar cells with chlorophyll derivatives and related natural porphyrins," *The Journal of Physical Chemistry*, vol. 97, no. 23, pp. 6272–6277, 1993.

[11] F. Odobel, E. Blart, M. Lagrée, et al., "Porphyrin dyes for TiO_2 sensitization," *Journal of Materials Chemistry*, vol. 13, no. 3, pp. 502–510, 2003.

[12] M. K. Nazeeruddin, R. Humphry-Baker, M. Grätzel, et al., "Efficient near-IR sensitization of nanocrystalline TiO_2 films by zinc and aluminum phthalocyanines," *Journal of Porphyrins and Phthalocyanines*, vol. 3, no. 3, pp. 230–237, 1999.

[13] J. He, A. Hagfeldt, S. E. Lindquist, et al., "Phthalocyanine-sensitized nanostructured TiO_2 electrodes prepared by a novel anchoring method," *Langmuir*, vol. 17, no. 9, pp. 2743–2747, 2001.

[14] W. Paw, S. D. Cummings, M. A. Mansour, W. B. Connick, D. K. Geiger, and R. Eisenberg, "Luminescent platinum complexes: tuning and using the excited state," *Coordination Chemistry Reviews*, vol. 171, no. 1, pp. 125–150, 1998.

[15] A. Islam, H. Sugihara, K. Hara, et al., "Dye sensitization of nanocrystalline titanium dioxide with square planar platinum(II) diimine dithiolate complexes," *Inorganic Chemistry*, vol. 40, no. 21, pp. 5371–5380, 2001.

[16] J. M. Rehm, G. L. McLendon, Y. Nagasawa, K. Yoshihara, J. Moser, and M. Grätzel, "Femtosecond electron-transfer dynamics at a sensitizing dye-semiconductor (TiO_2) interface," *Journal of Physical Chemistry*, vol. 100, no. 23, pp. 9577–9578, 1996.

[17] P. V. Kamat and W. E. Ford, "Photochemistry on surfaces: triplet-triplet energy transfer on colloidal TiO_2 particles," *Chemical Physics Letters*, vol. 135, no. 4-5, pp. 421–426, 1987.

[18] S. Das, C. S. Rajesh, C. H. Suresh, et al., "Photophysical and photoelectrochemical behavior of poly[styrene-co-3-(acrylamido)-6-aminoacridine]," *Macromolecules*, vol. 28, no. 12, pp. 4249–4254, 1995.

[19] D. Liu and P. V. Kamat, "Photoelectrochemical behavior of thin CdSe and coupled TiO_2/CdSe semiconductor films," *Journal of Physical Chemistry*, vol. 97, no. 41, pp. 10769–10773, 1993.

[20] M. K. Nazeeruddin, A. Kay, I. Rodicio, et al., "Conversion of light to electricity by cis-Xbis(2, 2′-bipyridyl-4, 4′-dicarboxylate)ruthenium(II) charge-transfer sensitizers (X = Cl, Br, I, CN, and SCN) on nanocrystalline TiO_2 electrodes," *Journal of the American Chemical Society*, vol. 115, no. 14, pp. 6382–6390, 1993.

[21] G. Sauvé, M. E. Cass, G. Coia, et al., "Dye sensitization of nanocrystalline titanium dioxide with osmium and ruthenium polypyridyl complexes," *Journal of Physical Chemistry B*, vol. 104, no. 29, pp. 6821–6836, 2000.

[22] P. Wang, C. Klein, R. Humphry-Baker, S. M. Zakeeruddin, and M. Grätzel, "A high molar extinction coefficient sensitizer for stable dye-sensitized solar cells," *Journal of the American Chemical Society*, vol. 127, no. 3, pp. 808–809, 2005.

[23] A. Hagfeldt and M. Grätzel, "Molecular photovoltaics," *Accounts of Chemical Research*, vol. 33, no. 5, pp. 269–277, 2000.

[24] F. Cecchet, A. M. Gioacchini, M. Marcaccio, et al., "Solvent effects on the oxidative electrochemical behavior of cis-bis(isothiocyanato)ruthenium(II)-bis-2, 2′-bipyridine-4, 4′-dicarb oxylic acid," *Journal of Physical Chemistry B*, vol. 106, no. 15, pp. 3926–3932, 2002.

[25] S. Altobello, R. Argazzi, S. Caramori, et al., "Sensitization of nanocrystalline TiO_2 with black absorbers based on Os and Ru polypyridine complexes," *Journal of the American Chemical Society*, vol. 127, no. 44, pp. 15342–15343, 2005.

[26] C. W. Lee, H. P. Lu, C. M. Lan, et al., "Novel zinc porphyrin sensitizers for dye-sensitized solar cells: synthesis and spectral, electrochemical, and photovoltaic properties," *Chemistry: A European Journal*, vol. 15, no. 6, pp. 1403–1412, 2009.

[27] X.-F. Wang, O. Kitao, H. Zhou, H. Tamiaki, and S.-I. Sasaki, "Efficient dye-sensitized solar cell based on oxo-bacteriochlorin sensitizers with broadband absorption capability," *Journal of Physical Chemistry C*, vol. 113, no. 18, pp. 7954–7961, 2009.

[28] W. M. Campbell, K. W. Jolley, P. Wagner, et al., "Highly efficient porphyrin sensitizers for dye-sensitized solar cells," *Journal of Physical Chemistry C*, vol. 111, no. 32, pp. 11760–11762, 2007.

[29] B. C. O'Regan, I. López-Duarte, M. V. Martínez-Díaz, et al., "Catalysis of recombination and its limitation on open circuit voltage for dye sensitized photovoltaic cells using phthalocyanine dyes," *Journal of the American Chemical Society*, vol. 130, no. 10, pp. 2906–2907, 2008.

[30] J.-H. Yum, P. Walter, S. Huber, et al., "Efficient far red sensitization of nanocrystalline TiO_2 films by an unsymmetrical squaraine dye," *Journal of the American Chemical Society*, vol. 129, no. 34, pp. 10320–10321, 2007.

[31] C. G. Garcia, A. Sarto Polo, and N. Y. Murakami Iha, "Fruit extracts and ruthenium polypyridinic dyes for sensitization of TiO_2 in photoelectrochemical solar cells," *Journal of Photochemistry and Photobiology A*, vol. 160, no. 1-2, pp. 87–91, 2003.

[32] G. Calogero and G. Di Marco, "Red Sicilian orange and purple eggplant fruits as natural sensitizers for dye-sensitized solar cells," *Solar Energy Materials and Solar Cells*, vol. 92, no. 11, pp. 1341–1346, 2008.

[33] T. A. Heimer, E. J. Heilweil, C. A. Bignozzi, and G. J. Meyer, "Electron injection, recombination, and halide oxidation dynamics at dye-sensitized metal oxide interfaces," *Journal of Physical Chemistry A*, vol. 104, no. 18, pp. 4256–4262, 2000.

[34] I. Montanari, J. Nelson, and J. R. Durrant, "Iodide electron transfer kinetics in dye-sensitized nanocrystalline TiO_2 films," *Journal of Physical Chemistry B*, vol. 106, no. 47, pp. 12203–12210, 2002.

[35] G. Schlichthörl, S. Y. Huang, J. Sprague, and A. J. Frank, "Band edge movement and recombination kinetics in dye-sensitized nanocrystalline TiO_2 solar cells: a study by intensity modulated photovoltage spectroscopy," *Journal of Physical Chemistry B*, vol. 101, no. 41, pp. 8141–8155, 1997.

[36] S. Y. Huang, G. Schlichthörl, A. J. Nozik, M. Grätzel, and A. J. Frank, "Charge recombination in dye-sensitized nanocrystalline TiO_2 solar cells," *Journal of Physical Chemistry B*, vol. 101, no. 14, pp. 2576–2582, 1997.

[37] H. Nusbaumer, J. E. Moser, S. M. Zakeeruddin, M. K. Nazeeruddin, and M. Grätzel, "Co(dbbip) complex rivals tri-iodide/iodide redox mediator in dye-sensitized photovoltaic cells," *Journal of Physical Chemistry B*, vol. 105, no. 43, pp. 10461–10464, 2001.

[38] C. Klein, M. K. Nazeeruddin, D. Di Censo, P. Liska, and M. Grätzel, "Amphiphilic ruthenium sensitizers and their applications in dye-sensitized solar cells," *Inorganic Chemistry*, vol. 43, no. 14, pp. 4216–4226, 2004.

[39] P. Wang, S. M. Zakeeruddin, P. Comte, R. Charvet, R. Humphry-Baker, and M. Grätzel, "Enhance the performance of dye-sensitized solar cells by Co-grafting amphiphilic sensitizer and hexadecylmalonic acid on TiO_2 nanocrystals," *Journal of Physical Chemistry B*, vol. 107, no. 51, pp. 14336–14341, 2003.

[40] S. A. Sapp, C. M. Elliott, C. Contado, S. Caramori, and C. A. Bignozzi, "Substituted polypyridine complexes of cobalt(II/III) as efficient electron-transfer mediators in dye-sensitized solar cells," *Journal of the American Chemical Society*, vol. 124, no. 37, pp. 11215–11222, 2002.

[41] T. N. Murakami, S. Ito, Q. Wang, et al., "Highly efficient dye-sensitized solar cells based on carbon black counter electrodes," *Journal of the Electrochemical Society*, vol. 153, no. 12, pp. A2255–A2261, 2006.

[42] E. Ramasamy, W. J. Lee, D. Y. Lee, and J. S. Song, "Spray coated multi-wall carbon nanotube counter electrode for tri-iodide (I_3^-) reduction in dye-sensitized solar cells," *Electrochemistry Communications*, vol. 10, no. 7, pp. 1087–1089, 2008.

[43] T. Denaro, V. Baglio, M. Girolamo, et al., "Investigation of low cost carbonaceous materials for application as counter electrode in dye-sensitized solar cells," *Journal of Applied Electrochemistry*, vol. 39, no. 11, pp. 2173–2179, 2009.

[44] C.-S. Chou, R.-Y. Yang, M.-H. Weng, and C.-I. Huang, "The applicability of SWCNT on the counter electrode for the dye-sensitized solar cell," *Advanced Powder Technology*, vol. 20, no. 4, pp. 310–317, 2009.

[45] P. J. Cameron and L. M. Peter, "Characterization of titanium dioxide blocking layers in dye-sensitized nanocrystalline solar cells," *Journal of Physical Chemistry B*, vol. 107, no. 51, pp. 14394–14400, 2003.

[46] L. G. Wade, *Organic Chemistry*, Prentice Hall, Englewood Cliffs, NJ, USA, 1991.

[47] S. Cazzanti, S. Caramori, R. Argazzi, C. M. Elliott, and C. A. Bignozzi, "Efficient non-corrosive electron-transfer mediator mixtures for dye-sensitized solar cells," *Journal of the American Chemical Society*, vol. 128, no. 31, pp. 9996–9997, 2006.

[48] K. Murakoshi, R. Kogure, Y. Wada, and S. Yanagida, "Fabrication of solid-state dye-sensitized TiO_2 solar cells combined with polypyrrole," *Solar Energy Materials and Solar Cells*, vol. 55, no. 1-2, pp. 113–125, 1998.

[49] S. Caramori, S. Cazzanti, L. Marchini, et al., "Dye-sensitized solar cells based on PEDOP as a hole conductive medium," *Inorganica Chimica Acta*, vol. 361, no. 3, pp. 627–634, 2008.

[50] D. Martineau, M. Beley, P. C. Gros, S. Cazzanti, S. Caramori, and C. A. Bignozzi, "Tuning of ruthenium complex properties using pyrrole- and pyrrolidine-containing polypyridine ligands," *Inorganic Chemistry*, vol. 46, no. 6, pp. 2272–2277, 2007.

[51] E. Palomares, J. N. Clifford, S. A. Haque, T. Lutz, and J. R. Durrant, "Slow charge recombination in dye-sensitised solar cells (DSSC) using Al_2O_3 coated nanoporous TiO_2 films," *Chemical Communications*, no. 14, pp. 1464–1465, 2002.

[52] Y. Kim, Y. E. Sung, J. B. Xia, M. Lira-Cantu, N. Masaki, and S. Yanagida, "Solid-state dye-sensitized TiO_2 solar cells using poly(3,4-ethylenedioxythiophene) as substitutes of iodine/iodide electrolytes and noble metal catalysts on FTO counter electrodes," *Journal of Photochemistry and Photobiology A*, vol. 193, no. 2-3, pp. 77–80, 2008.

[53] C. M. Elliott, S. Caramori, and C. A. Bignozzi, "Indium tin oxide electrodes modified with tris(2,2′-bipyridine-4,4′-dicarboxylic acid) iron(II) and the catalytic oxidation of tris(4,4′-di-tert-buty1-2,2′-bipyridine) cobalt(II)," *Langmuir*, vol. 21, no. 7, pp. 3022–3027, 2005.

[54] M. J. Scott, J. J. Nelson, S. Caramori, C. A. Bignozzi, and C. M. Elliott, "cis-dichloro-bis(4,4′-dicarboxy-2,2-bipyridine)osmium(II)-modified optically transparent electrodes: application as cathodes in stacked dye-sensitized solar cells," *Inorganic Chemistry*, vol. 46, no. 24, pp. 10071–10078, 2007.